Available online at www.sciencedirect.com
SCIENCE DIRECT
ELSEVIER
Ultramicroscopy 106 (2006) 808–814
ultramicroscopy
www.elsevier.com/locate/ultramic

A femtogram resolution mass sensor platform based on SOI electrostatically driven resonant cantilever. Part II: Sensor calibration and glycerine evaporation rate measurement

J. Teva[a,*], G. Abadal[a], F. Torres[a], J. Verd[a], F. Pérez-Murano[b], N. Barniol[a]

[a]*Dept. d'Enginyeria Electrònica, Universitat Autònoma de Barcelona, Bellaterra E- 08193, Spain*
[b]*Institut de Microelectrònica Barcelona (IMB-CNM) Campus UAB, Bellaterra E-08193, Spain*

Received 3 October 2005; accepted 28 December 2005

Abstract

This paper presents mass measurements of glycerine beads performed by means of laterally resonant micro-cantilevers. The transducer architecture is based on a resonant cantilever electrostatically coupled by two parallel placed electrodes. Previous to glycerine measurements, a calibration of the mass sensor has been performed by measuring a standard mass based on latex spheres. From these measurements, a value of the mass responsivity is deduced. In addition, a study of the transducer phase noise has been carried out in order to determine the minimum detectable mass. Mass measurements experiments have been performed by detecting the change on the resonance frequency of the on-plane cantilever resonant mode, produced by locally deposited mass. Additionally, the mass losses detected on the calibrated transducer after glycerine drop deposition allowed determining its evaporation rate.

PACS: 77.65.Fs; 83.85.Gk; 85.40.Ux; 07.10.Cm.

Keywords: MEMS; Cantilever based sensors; Mass sensor; Evaporation rate

1. Introduction

Cantilever based sensors have been demonstrated to be a robust platform for different applications in physical and chemical domains [1–3]. For mass detection, it has been demonstrated that with the dynamic mode of operation a high mass resolution can be achieved [4]. One possible dynamic configuration consists of exciting electrostatically the cantilever, by means of a close parallel structure—driver electrode- (see Fig. 1), and reading the generated capacitive current. Reducing the dimensions allows increasing the mass responsivity. However, when reducing the dimensions some problems arise due to the low-level current generated combined with the parasitic capacitance. In order to reduce these parasitic capacitances and then, to be able to detect these low–level generated current, a CMOS circuitry is designed and placed very close to the transducer structure. Huge effort has been done in order to integrate MEMS structures defined by nanolithography techniques (EBL, AFM-lithography) with CMOS circuitry [5–6], obtaining successful first prototypes. Nevertheless, the compatibilization of nanofabrication and CMOS process implies as many critical steps that results in a low final device production yield. In this framework, having a robust, versatile and easy-to-fabricate structure allows having enough devices for testing, despite of loosing mass responsivity. The test-structure allows defining, in a first instance, a right mass measurement protocol for afterwards transferring this experience to those high-resolution structures.

In the present paper, mass measurements have been performed by a mass standard based on latex spheres

*Corresponding author. Tel.: +34 93 581 3514; fax: +34 93 581 2600.
E-mail address: Jorge.Teva@uab.es (J. Teva).

0304-3991/$ - see front matter © 2006 Elsevier B.V. All rights reserved.
doi:10.1016/j.ultramic.2005.12.017

1 μm in diameter, in order to characterize the sensor mass responsivity. These measurements are accompanied by a phase stability study in order to determine the maximum achievable mass resolution. Once the transducer is characterized, in situ mass measurements of a volatile analyte have been performed, leading to an evaporation rate value for a glycerine bead.

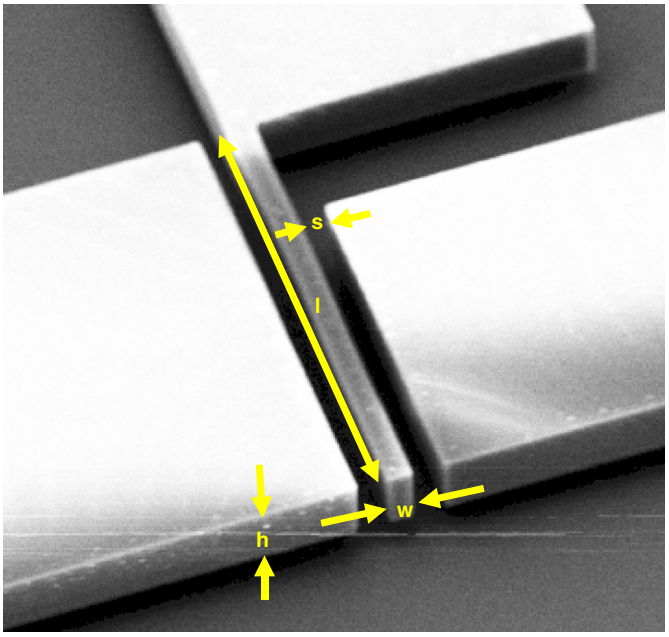

Fig. 1. SEM image of the cantilever-driver structure (CDS) showing the geometrical parameters: length (l), width (w), thickness (h), cantilever–driver gap distance (s). The dimensions of the structure are: $l = 40\,\mu m$, $w = 2.3\,\mu m$, $h = 5\,\mu m$ and $s = 2.4\,\mu m$.

2. Transducers and Experimental Setup

Doped silicon cantilever with double driver structures and contact pads for external connection have been fabricated by optical lithography on SOI substrates [7] (see Fig. 1). Scanning electron microscopy (SEM) has been used to determine the cantilever-driver dimensions. The lateral vibrating cantilevers are 40 μm in length (l), 5 μm in thickness (h) and 2.3 μm in width (w). The gap distance between drivers and cantilever (s) is around 2.4 μm. The configuration used in the experiments is also shown in Fig. 2. One of the electrodes is used to apply the ac signal and the other is used to collect the output current generated in the transducer. The ac signal applied on the driver electrode excites electrostatically the cantilever carrying it to resonance. The dc bias voltage is applied at the cantilever. On the other electrode, the capacitive current generated is measured by means of a network analyzer, *Agilent E5100A*. The current generated is given by the following equation:

$$I \propto V_{DC}\frac{dC}{dt} + C_{Trhu}\frac{dV_{AC}(t)}{dt}, \quad (1)$$

defining C_{Trhu} as the parasitic capacitance between the driver and readout electrodes, and dC/dt as the time-variable cantilever–read out driver capacitance. The first term in Eq. (1) is due to the cantilever resonance which is reflected in the capacitance variation term. The second term in Eq. (1) represents a parasitic signal that has to be minimized to be able to detect the resonance peak. The chosen experimental configuration allows reducing significantly that parasitic capacitance, because there is not direct coupling between the driver and the readout electrode. In fact, C_{Trhu} is reduced to be the fringing field capacitance

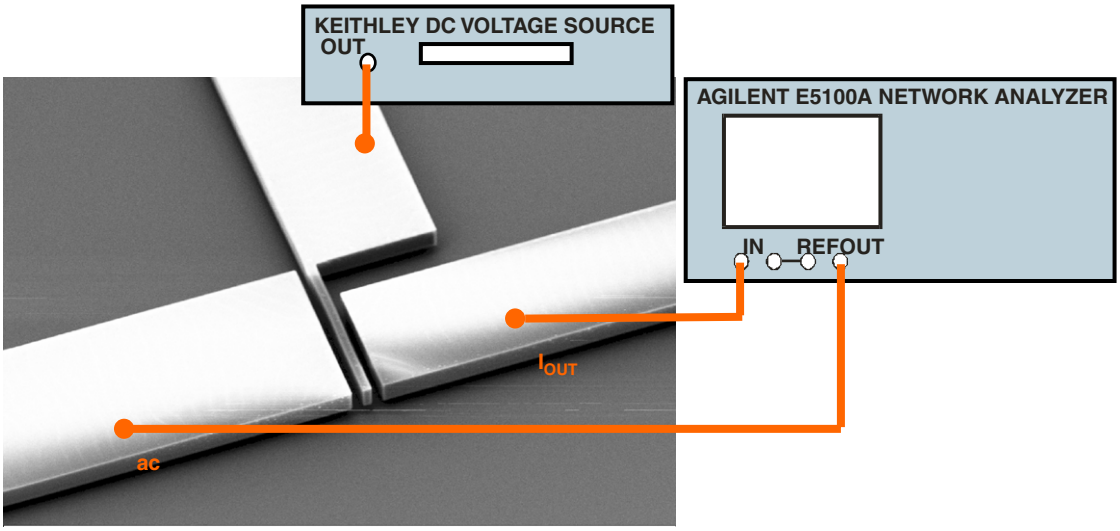

Fig. 2. Experimental configuration for electrical resonance curve measurements. One electrode is used to connect the ac input signal, while the other electrode is connected to the input port of the network analyzer. The dc bias voltage is connected to the cantilever electrode.

between the two electrodes [8]. Also, the configuration avoids summing up the dc and ac voltages.

Measurements of the magnitude and phase curves of the S_{21} parameter near cantilever resonance have been performed in ambient air. The resonance frequency is determined by these measurements. The polarization conditions for all the experiments have been fixed to be $V_{DC} = 100\,V$, and the ac power driving signal of $P_{in} = 18\,dBm$. Electrical contact to the cantilever and driver electrodes has been made by means of one independent conventional probe with 3-axial micro-positioning and a probe chart.

3. Sensor calibration

The mass sensor proposed is operating in the dynamic mode near resonance. When a change of mass is induced in the vibrating cantilever the resonance frequency decreases, giving a mass responsivity of

$$\Re^{-1} = \left|\frac{dm}{df}\right| = \frac{k}{2\pi^2 f^3} \quad \left(\mathrm{kg}\Big/\mathrm{Hz}\right), \tag{2}$$

where k and f are the equivalent spring constant and resonance frequency of the cantilever transducer:

$$k = \frac{E}{4}\frac{w^3}{l^3}h \quad \left(\mathrm{N}\Big/\mathrm{m}\right), \tag{3}$$

$$f = \frac{1}{2\pi}\sqrt{\frac{E}{\rho}}\frac{w}{l^2} \quad (\mathrm{Hz}), \tag{4}$$

where w, l, h are the cantilever width, length and thickness (Fig. 1). E and ρ are the doped silicon Young modulus and mass density, respectively. From our measurements [7], material properties are determined to be $E = 120\,GPa$ and $\rho = 2.33e3\,kg/m^3$. Then, from these values and the geometrical dimensions, the theoretical mass sensitivity is determined to be (Eq. (1)):

$$\left|\frac{dm}{df}\right|_{THEO} = 0.3 fg/Hz. \tag{5}$$

In order to check experimentally this sensitivity, a standard mass has been measured. The standard mass chosen is a latex sphere of 500 nm of radius, with a well-known density, ($\rho_{LATEX} = 1.05\,kg/m^3$) and mass of $dm = 549\,fg$ [9]. Two different calibration experiments have been carried out consisting on the deposition of latex spheres at the free end of the cantilever. The deposition of the latex spheres on the cantilever surface has been done by softly contacting with a tungsten STM tip, which is controlled by a simple micropositioner. The inset of Fig. 3 shows a SEM image of the cantilever free end, after the latex sphere deposition process. As it can be seen, one latex sphere 1 μm in diameter is deposited at the cantilever free end. Experimental S_{21} parameter curves have been measured before and after the mass deposition by the E5100A network analyzer. Fig. 3 shows the frequency shift before and after the mass deposition corresponding to the magnitude and phase measured at the input port of the network analyzer. In order to reduce the frequency shift measurement error, the criteria to establish the frequency shift has been chosen as the minimum of the phase. The frequency shift measured is $|df| = 2\,kHz$ corresponding to a deposited mass of $dm = 549\,fg$. Then, the experimental mass

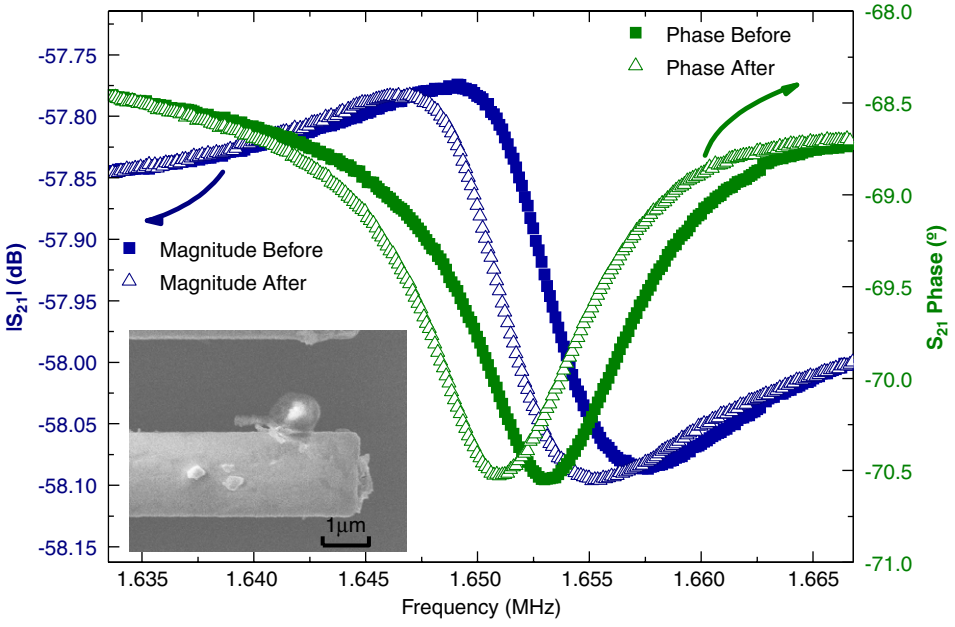

Fig. 3. Transducer's output current measured at the E5100A network analyzer before and after one latex sphere deposition. Experimental frequency resonance measurement is shown by means of the magnitude and phase of the S_{21} transmission signal. The inset of the figure shows a SEM image of the free end cantilever with the deposited latex sphere.

sensitivity is

$$\left|\frac{\mathrm{d}m}{\mathrm{d}f}\right|_{\mathrm{EXP},m1} = 0.27\mathrm{fg/Hz}$$

which is in accordance with the theoretical one (Eq. (5)).

As it can be seen in the inset of Fig. 3, some additional mass located at the STM tip is also accidentally deposited when adding the latex sphere to the cantilever surface. This can result in a larger change in the resonance frequency than expected, lowering the mass sensitivity measurement. The second experiment has been performed in a similar structure, but depositing three latex spheres. Fig. 4 shows the SEM image after a latex sphere deposition at the cantilever free end. In that case, the frequency shift measured was $|\mathrm{d}f| = 5.45\,\mathrm{kHz}$ and the mass deposited is $\mathrm{d}m = 3 \times 549\,\mathrm{fg} = 1647\,\mathrm{fg}$. In that case, the mass sensitivity is determined to be

$$\left|\frac{\mathrm{d}m}{\mathrm{d}f}\right|_{\mathrm{EXP},m2} = 0.30\mathrm{fg/Hz}$$

which is in accordance with the theoretical value. For this reason, and for the further experiments, the mass sensitivity is chosen to be:

$$\left|\frac{\mathrm{d}m}{\mathrm{d}f}\right| = 0.3\mathrm{fg/Hz}. \quad (6)$$

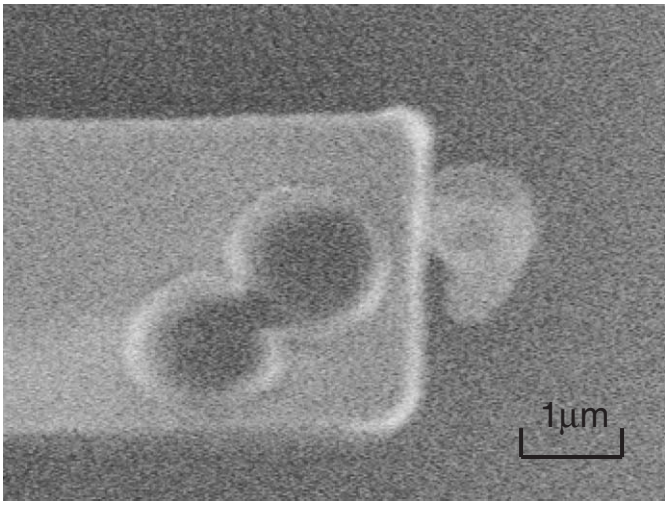

Fig. 4. SEM image corresponding to the three latex spheres depicted at the cantilever free end.

4. Sensor resolution

Sensor resolution is defined as the minimum detectable mass, δm_{min}, that can be simply evaluated from the transducer responsivity, Eq. (2), and from the minimum detectable resonance frequency shift, $\delta f_{\mathrm{RES_{min}}}$, by

$$\delta m_{\mathrm{min}} = \Re^{-1} \times \delta f_{\mathrm{RES_{min}}}. \quad (7)$$

The minimum detectable resonance frequency shift has been determined experimentally in order to take into account the contributions to this parameter of all the set-up and ambient conditions. We assume that the shift in resonance frequency is obtained through the change of phase signal measured at constant excitation frequency.

From the measured frequency response of the electrical signal near the resonance, Fig. 5, the phase slope of the linear region around resonance can be

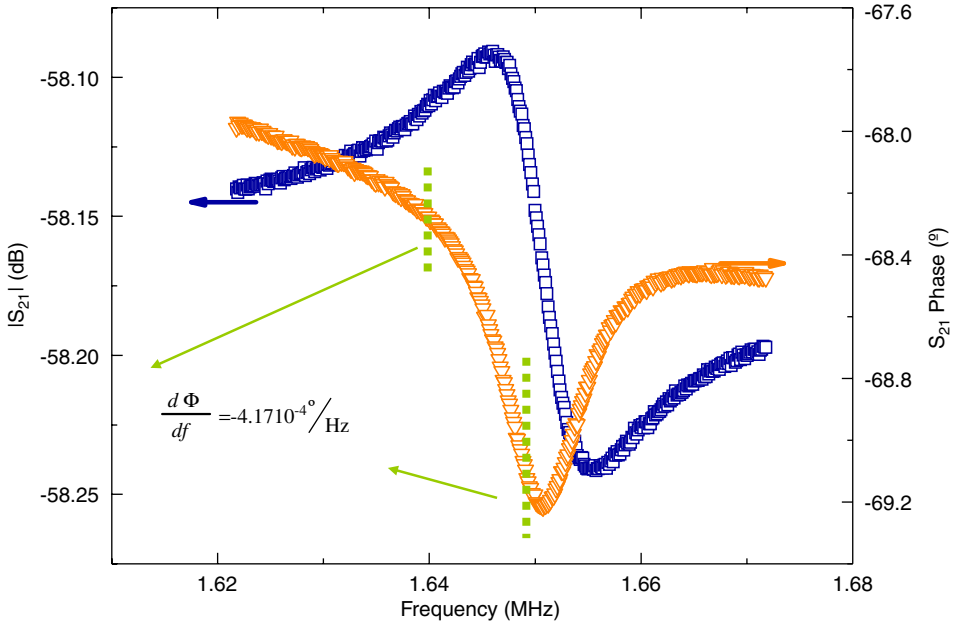

Fig. 5. S_{21} transmission signal measurement near cantilever resonance for the phase versus frequency ($\mathrm{d}\phi/\mathrm{d}f$) slope determination.

determined to be:

$$\left|\frac{d\Phi}{df}\right| = 4.17 \times 10^{-4}\text{Hz}. \quad (8)$$

In order to know the resolution in f_{RES}, the maximum $d\Phi$ fluctuation has to be found, once $d\Phi/df$ is determined. For this purpose, a study of the phase evolution at a fixed frequency has been performed. The frequency chosen is 1.644776 MHz that corresponds to the centre of the linear region. The network analyzer works, then, as an oscilloscope, measuring the phase evolution versus time, as shown in Fig. 6. From that measurement, the phase noise is determined to be $d\Phi_{MIN} = 0.04^\circ$, which implies a frequency shift given by

$$df_{\text{MIN}} = \frac{1}{\left|d\Phi \Big/ df\right|} d\Phi_{\text{MIN}} = 95.9\text{Hz}, \quad (9)$$

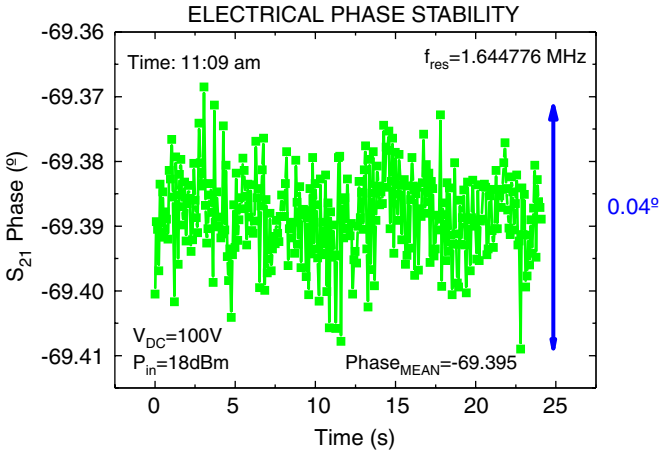

Fig. 6. Measurement of the phase evolution versus time at fixed frequency. The short-time variation of the phase is 0.04°.

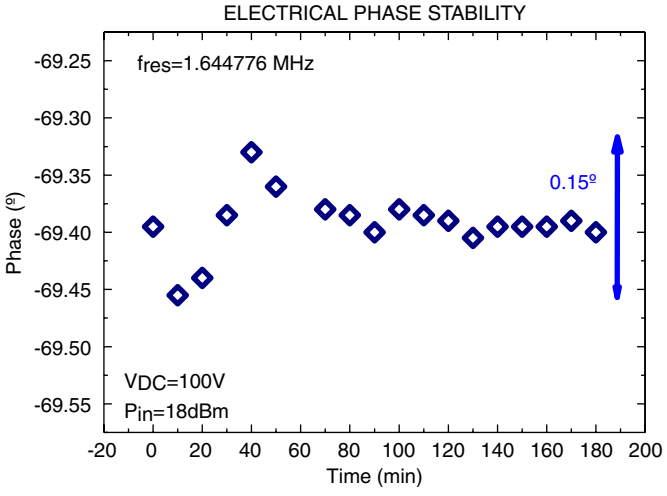

Fig. 7. Graph showing the phase mean value evolution. This value varies in an interval of 0.15°, thus limiting the mass resolution of the sensor.

which combined with (6) implies a maximum mass resolution of 28.7 fg.

The phase behaviour also presents long-time fluctuations, due to thermo elastic fluctuations inherent to the transducer properties [10–11]. Phase fluctuations have been studied during three hours, see Fig. 7, measuring fluctuations within the range of 0.15°, yielding a mass resolution of 107.9 fg. So, long-time instabilities reduce considerably the sensor maximum mass resolution from 28.7 to 107.9 fg.

5. Glycerine measurements

The previous calibration performance has allowed having a very-well characterized mass responsivity. Now, the aim is to measure in situ the evaporation rate of a micro-glycerine bead. The bead is placed near the cantilever free end in order to have more sensitivity. Electrical measurements have been carried out before and after the bead deposition in order to measure the change on the resonance frequency, Fig. 8. In that case, the resonance frequency has been determined at a phase of value −72.5°, obtaining resonance frequencies of 1645.5 and 1642.5 kHz for before and after mass deposition, respectively. The experimental measurement of the change on the resonance frequency was $|df| = 3$ kHz. The deposited mass is then deduced from this value and from the measured mass sensitivity by the expression:

$$dm = \left|\frac{dm}{df}\right| \cdot df = 0.3 \times 310^3\text{fg} = 900\text{fg}. \quad (10)$$

The resonance frequency versus time has been plotted in Fig. 9 in order to study the glycerine bead mass evolution. The first two points correspond to the resonance frequency before and after the bead deposition. After approximately 2 min from the bead deposition a new measurement was carried out, measuring a resonance frequency of 1643.5 kHz (always maintaining the same measurement criteria, i.e., phase = −72.5°), see Fig. 9. The resonance frequency had increased, that means that the deposited mass had decreased between the two last experiments. Insets of Fig. 9 show optical images of the evaporating mass. The evaporated mass was calculated from the change on the resonance frequency, obtaining an evaporated mass of 300 fg. Afterwards, two more measurements were performed spaced one minute on time, obtaining resonance frequencies of 1644.5 and 1645 kHz, respectively, as shown in Fig. 9. From the resonance frequency evolution, the evaporation rate for the glycerine is extracted. Firstly, and by a linear fit, the resonance frequency evolution versus time is determined, obtaining 10.7 Hz/s. Then, the evaporation rate, calculated via that value and the mass sensitivity, is

$$|dm/dt| = \left|\frac{dm}{df}\right| \times df/dt = 0.3 \times 10.7\text{fg/s} = 3.2\text{fg/s}. \quad (11)$$

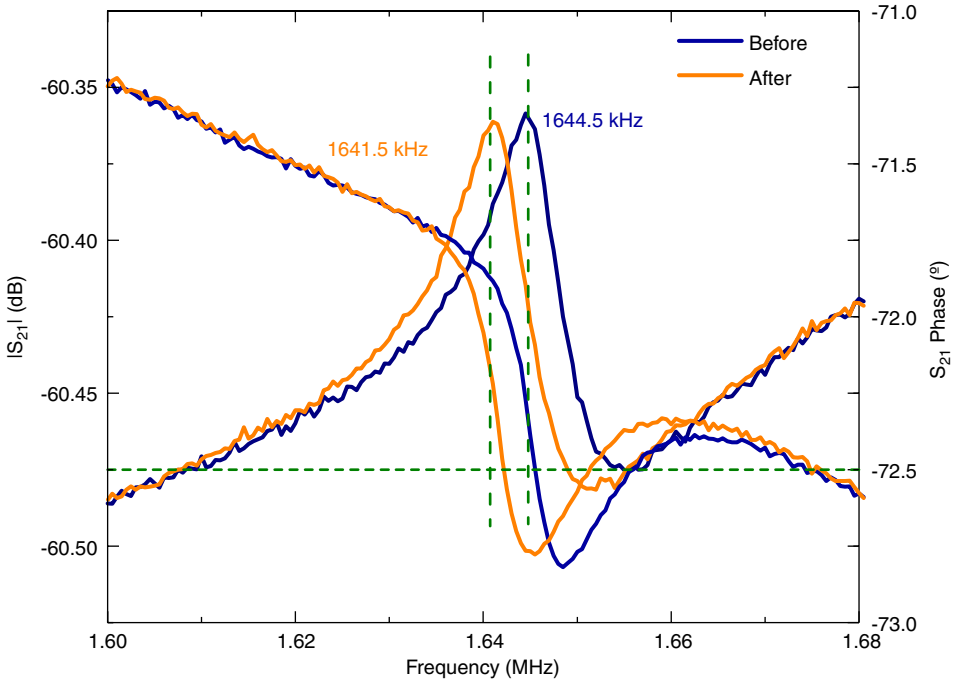

Fig. 8. S_{21} transmission signal measurement before and after the glycerine bead deposition. The change on the resonant frequency is measured at phase equal $-72.5°$.

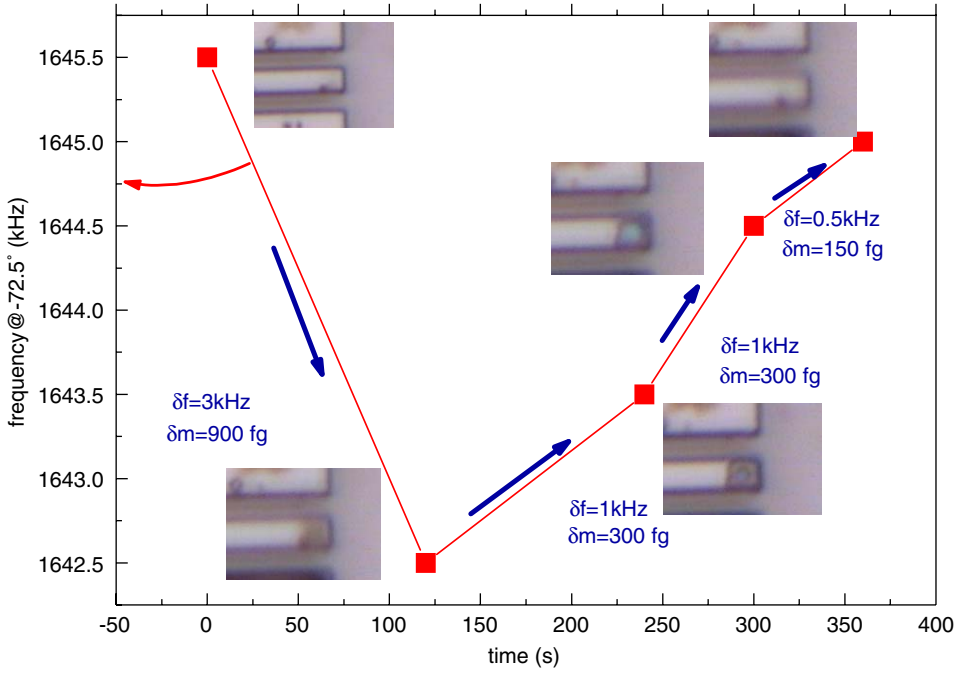

Fig. 9. Representation of the change on the resonance frequency evolution versus time, showing the calculated evaporating mass. The insets of the figure show optical images of the glycerine bead evaporation corresponding to each electrical measurement.

6. Conclusions

A robust cantilever mass based sensor has been fabricated, fully characterized and used as a test platform for mass measurements. A complete calibration using a standard mass based on micro-latex spheres has been performed, resulting in a very-well mass sensor characterization with a mass sensitivity of 0.3fg/Hz. The mass sensitivity calibration has been accompanied by a sensor noise and fluctuation study. This study, based on the registration of the phase changes near electrical resonance has allowed establishing the maximum mass sensor resolution value near 100 fg. Upon these results, the mass evolution of a volatile system has been measured, allowing

monitorizing in situ the change of mass. The evaporation rate for a glycerine bead of 900 fg has been deduced from the transitory changes of mass, giving a value of 3.2 fg/Hz. So, the transducer introduced has become a robust platform to study the glycerine bead deposition and evaporation and furthermore, arises as an alternative way to integrated sensors for sensing mass above the femtogram range.

Acknowledgement

This work has been partially supported by the projects NANOMASS II (EU-IST-2001-33068) and NANOSYS (MYCT-TIC2003-0723).

References

[1] K.L. Ekinci, M.L. Roukes, Rev. of Scient. Instrum. 76 (2005) 061101.
[2] N.V. Lavrik, M.J. Sepaniak, P.G. Datskos, Rev. of Scient. Instrum. 75 (7) (2004) 2229–2253.
[3] R. Berger, Ch. Gerber, H.P. Lang, J.K. Gimzewski, Microelectron Eng 35 (1997) 373.
[4] K.L. Ekinci, X.M.H. Huang, M.L. Roukes, Appl. Phys. Lett. 84–22 (2004) 4469.
[5] J. Verd, G. Abadal, JTeva, M. Villarroya, A. Uranga, X. Borrisé, F. Campabadal, J. Esteve, E. Figueras, FPérez-Murano, Z.J. Davis, E. Forsén, A. Boisen, N. Barniol, IEEE J. Microelectromech. Systems 14 (2005) 508.
[6] E. Forsén, G. Abadal, S. Ghatnekar-Nilsson, J. Teva, J. Verd, R. Sandberg, W. Svendsen, F. Pérez-Murano, J. Esteve, E. Figueras, F. Campabadal, L. Montelius, N. Barniol, A. Boisen. Appl. Phys. Lett. 87 (2005) 043507.
[7] J. Teva, G. Abadal, F.Torres, J. Verd, F. Pérez-Murano, N. Barniol. Ultramicroscopy, in press, doi:10.1016/j.ultramic.2005.12.016.
[8] J. R. Clark, W.-T. Hsu, and C. T.-C. Nguyen, Technical Digest, IEEE International Electron Devices Meeting, San Francisco, California, December 11–13, 2000 pp. 493.
[9] Polybead Amino Microspheres 1 μm. Polysciences. Inc.
[10] B. Razavi, IEEE J. solid-state circuit. 31 (1996) 331.
[11] T.B. Gabrielson, IEEE Trans. Ele. Dev. 40 (5) (1993) 903.